INFECTIOUS DISEASE

RNAi-based treatment of chronically infected patients and chimpanzees reveals that integrated hepatitis B virus DNA is a source of HBsAg

Christine I. Wooddell,[1]*† Man-Fung Yuen,[2]* Henry Lik-Yuen Chan,[3] Robert G. Gish,[4] Stephen A. Locarnini,[5,6] Deborah Chavez,[7] Carlo Ferrari,[8,9] Bruce D. Given,[1] James Hamilton,[10] Steven B. Kanner,[1] Ching-Lung Lai,[2] Johnson Y. N. Lau,[11] Thomas Schluep,[10] Zhao Xu,[1] Robert E. Lanford,[7] David L. Lewis[1]

Chronic hepatitis B virus (HBV) infection is a major health concern worldwide, frequently leading to liver cirrhosis, liver failure, and hepatocellular carcinoma. Evidence suggests that high viral antigen load may play a role in chronicity. Production of viral proteins is thought to depend on transcription of viral covalently closed circular DNA (cccDNA). In a human clinical trial with an RNA interference (RNAi)–based therapeutic targeting HBV transcripts, ARC-520, HBV S antigen (HBsAg) was strongly reduced in treatment-naïve patients positive for HBV e antigen (HBeAg) but was reduced significantly less in patients who were HBeAg-negative or had received long-term therapy with nucleos(t)ide viral replication inhibitors (NUCs). HBeAg positivity is associated with greater disease risk that may be moderately reduced upon HBeAg loss. The molecular basis for this unexpected differential response was investigated in chimpanzees chronically infected with HBV. Several lines of evidence demonstrated that HBsAg was expressed not only from the episomal cccDNA minichromosome but also from transcripts arising from HBV DNA integrated into the host genome, which was the dominant source in HBeAg-negative chimpanzees. Many of the integrants detected in chimpanzees lacked target sites for the small interfering RNAs in ARC-520, explaining the reduced response in HBeAg-negative chimpanzees and, by extension, in HBeAg-negative patients. Our results uncover a heretofore underrecognized source of HBsAg that may represent a strategy adopted by HBV to maintain chronicity in the presence of host immunosurveillance. These results could alter trial design and endpoint expectations of new therapies for chronic HBV.

INTRODUCTION

Globally, an estimated 250 million to 400 million people are chronically infected with hepatitis B virus (HBV), and about 1 million die each year from HBV-related liver disease (*1*, *2*). HBV is transmitted parenterally and infects hepatocytes. The immune system mounts an effective immune response that controls the virus in 95% of patients infected as adults. In contrast, infected neonates and young children usually become chronically HBV infected (CHB) after exposure. When untreated, 40% of men and 15% of women infected early in life later die of cirrhosis or hepatocellular carcinoma (HCC) or require liver transplantation (*3*).

The HBV virion contains a compact 3.2-kb genome that exists as a partially double-stranded, relaxed circular DNA (rcDNA) with a 7- to 9-base terminal redundancy that is converted into covalently closed circular DNA (cccDNA) within the nucleus of the hepatocyte, functioning as a minichromosome for HBV transcription (*4*). Host RNA polymerase II transcribes HBV genes on the cccDNA to produce five viral RNAs: transcripts that encode precore [serologically called HBV e antigen (HBeAg)], the pregenomic RNA (pgRNA) that encodes the structural capsid protein (core) and polymerase and is reverse-transcribed to produce rcDNA, the pre-S1 transcript that encodes the large S surface protein, another transcript that encodes pre-S2 and S surface proteins (middle and small S), and the X gene mRNA. The three surface proteins collectively comprise HBsAg. All HBV transcripts are encoded in overlapping reading frames, have a common 3′ end, and use the same polyadenylation signal (PAS). HBsAg, in a lipid bilayer, forms an envelope around each core-encapsidated, partially double-stranded HBV genome.

Although cccDNA is considered the driver of HBV transcription and replication, HBV DNA may integrate into the host genome, which has been associated with the development of HCC, may disrupt host genes or change their transcription levels, and may result in oncogenic fusion proteins (*5*, *6*). Integrated HBV genomes are found in non-HCC liver tissue of patients as well as in tumors (*7*). The amount of cccDNA is higher in HBeAg-positive than in HBeAg-negative patients (*8*), whereas amounts of integrated HBV are higher in HBeAg-negative patients (*7*). The primary source of integrated HBV DNA is likely double-stranded linear HBV DNA (dslDNA), arising as an aberrant replication product due to mispriming of (+) strand synthesis (*9*). Although integrated HBV DNA is associated with HCC, its function in the maintenance of HBV infection is unknown.

HBeAg and HBsAg play important roles in chronic infection (*10*). HBeAg is thought to induce T cell tolerance to HBeAg and core, which may contribute to viral persistence (*11*). This tolerance also predisposes the infant of an HBeAg-positive mother to allow persistent replication after infection (*12*). High HBsAg production is believed to contribute to T cell exhaustion, resulting in limited or weak T cell responses and even

[1]Arrowhead Pharmaceuticals, 502 South Rosa Road, Madison, WI 53719, USA. [2]Department of Medicine, University of Hong Kong, Queen Mary Hospital, Hong Kong, China. [3]Department of Medicine and Therapeutics and Institute of Digestive Disease, Chinese University of Hong Kong, Hong Kong, China. [4]Liver Transplant Program, Stanford University Medical Center, San Diego, CA 92037, USA. [5]Victorian Infectious Diseases Reference Laboratory, Melbourne, Victoria 3000, Australia. [6]WHO Regional Reference Laboratory for Hepatitis B, Doherty Institute, Melbourne, Victoria, Australia. [7]Southwest National Primate Research Center, Texas Biomedical Research Institute, San Antonio, TX 78227, USA. [8]Unit of Infectious Diseases and Hepatology, University of Parma, Parma 43126, Italy. [9]Azienda Ospedaliero-Universitaria of Parma, Parma 43126, Italy. [10]Arrowhead Pharmaceuticals, 225 South Lake Avenue, Suite 1050, Pasadena, CA 91101, USA. [11]Hong Kong Polytechnic University, Hong Kong, China.
*These authors contributed equally to this work.
†Corresponding author. Email: cwooddell@arrowheadpharma.com

deletion of T cells recognizing specific epitopes (*13*–*15*). In addition to enveloping the virion, HBsAg forms as many as 100,000 times more subviral particles than virions (*16*). For CHB patients, the desired endpoint of treatment is seroclearance of HBsAg, referred to as a "functional cure," resulting in improved long-term prognosis (*17*, *18*). HBsAg loss is considered a hallmark of effective immune control of HBV (*19*).

Because high antigen load is believed to play a key role in maintaining chronicity, there is interest in directly reducing expression of viral antigens and regulatory proteins via RNA interference (RNAi) (*20*). The RNAi therapeutic ARC-520 for treatment of chronic HBV infection comprises an equimolar mixture of liver-tropic cholesterol-conjugated small interfering RNAs (siRNAs) siHBV-74 and siHBV-77 plus an excipient that enables endosomal escape of the siRNAs into the cytoplasm where RNAi occurs (*21*). The mRNA target sites for siHBV-74 and siHBV-77 are 118 and 71 bases upstream, respectively, of the conventional HBV PAS (fig. S1). Because all cccDNA-derived HBV transcripts overlap in this region, the siRNAs in ARC-520 would target all of them, leading to reduction of all viral proteins. This would potentially enable a host immune response that would result in functional cure.

Here, we report results evaluating ARC-520 in a phase 2 clinical study in CHB patients and a complementary study in chimpanzees chronically infected with HBV. Our studies reveal a previously underappreciated source of HBsAg, namely, HBV DNA integrated into the host genome. This has implications for our understanding of HBV biology and host interactions and for future development of drugs designed with curative intent for CHB patients.

RESULTS

Differential reduction of HBsAg is associated with HBeAg status and previous exposure to NUCs in CHB patients treated with ARC-520

Heparc-2001 was a phase 2 clinical study to determine the safety and tolerability of ARC-520 and its effect on virologic parameters. Individual and mean patient demographics at study start are presented in tables S1 and S2, respectively. Initially, CHB patients receiving long-term entecavir (ETV) were enrolled into five 8-patient cohorts and randomized with a 6:2 (active/placebo) ratio. Patients in cohorts 1 to 4 were HBeAg-negative, whereas patients in cohort 5 were HBeAg-positive. ARC-520 was administered as a single intravenous infusion in cohorts 1 to 4, at ascending doses of 1, 2, 3, and 4 mg/kg, whereas patients in cohort 5 received 4 mg/kg. A sixth cohort of HBeAg-positive patients received two doses of ARC-520 (2 mg/kg) 2 weeks apart. Cohorts 1 to 6 had been on nucleos(t)ide viral replication inhibitors (NUCs) for 1.2 to 7.8 years before ARC-520 dosing. HBV serum DNA was below the lower limit of quantitation (<LLOQ) in these patients (table S2). Finally, a seventh, open-label cohort was added, which consists of HBeAg-negative and HBeAg-positive patients who were NUC-naïve. Daily ETV was initiated on the same day they received a single dose of ARC-520 (4 mg/kg). Mean baseline expression of HBsAg was similar between all cohorts (tables S1 and S2). A total of 58 CHB patients were successfully dosed in cohorts 1 to 7 of the study, with 48 receiving drug and 10 receiving placebo. There were few adverse events reported (table S3). No adverse trends were observed in vital signs, physical examinations, or electrocardiograms. Laboratory values showed no clinically significant toxicity. Overall, ARC-520 was well tolerated when administered to CHB patients, as it was in normal volunteers (*20*).

We observed modest decreases in HBsAg expression in cohort 1 to 4 patients that correlated partially with dose (Fig. 1A). HBsAg expression decreased most sharply during the first 8 days after dosing in all cohorts, reaching a plateau before starting to relapse 6 to 8 weeks after dosing. At the highest dose of 4 mg/kg (cohort 4), HBsAg was reduced by 0.3 $\log_{10}$ relative to baseline. This degree of knockdown was substantially less than observed in preclinical studies using a mouse model of HBV infection (*21*). The mice were HBeAg-positive; however, the HBeAg status of the patients did not appear to be a factor, because cohort 5 (HBeAg-positive) patients showed a similar muted response for HBsAg knockdown (Fig. 1B). Similar results from administration of two injections of 2 mg/kg 2 weeks apart in cohort 6, instead of a single dose (4 mg/kg), indicated that saturation of hepatocyte delivery of ARC-520 was an unlikely explanation for the limited HBsAg knockdown and minimal dose responsiveness (fig. S2).

The lack of robust HBsAg knockdown was unlikely due to inherent RNAi inefficiency or lack of ARC-520 efficacy in the CHB patients, as evidenced by measuring knockdown of other viral parameters. For example, measurement of hepatitis B core–related antigen (HBcrAg) in cohort 1 to 4 patients with quantifiable amounts showed dose-dependent knockdown, reaching 0.9 $\log_{10}$ mean reduction in patients receiving 4 mg/kg (Fig. 1C). Similar results were observed in cohort 5, with mean HBcrAg reduction of 0.9 $\log_{10}$ and HBeAg reduction of 1.2 $\log_{10}$ at nadir (Fig. 1D).

Cohorts 1 to 6 comprised patients who had been on long-term NUC therapy. To understand whether previous NUC therapy affected HBsAg reduction after ARC-520 injection, an additional cohort consisting of NUC-naïve patients (cohort 7) was studied. Six of these patients were HBeAg-positive and six were HBeAg-negative, but one of the positive patients had low HBeAg [<10 Paul Ehrlich Institut units (PEIU)/ml] and was considered to be transitioning to HBeAg-negative status. Cohort 7 patients received a single dose of ARC-520 (4 mg/kg) and began daily ETV dosing on day 1. HBV serum DNA in cohort 7 patients was higher at baseline in the HBeAg-positive (8 to 9 $\log_{10}$ IU/ml, excluding the low HBeAg-positive patient) than HBeAg-negative (3 to 5 $\log_{10}$) patients (table S1). HBV DNA production decreased in HBeAg-positive patients by 4.0 ± 0.6 $\log_{10}$ during the first 3 weeks of ARC-520 plus NUC treatment and became undetectable in most HBeAg-negative patients (fig. S3).

Excluding the transitional patient, NUC-naïve HBeAg-positive patients in cohort 7 responded with deep HBsAg reduction: A 1.4 ± 0.1 $\log_{10}$ reduction in HBsAg (minimum of 1.3 $\log_{10}$ and a maximum of 1.8 $\log_{10}$ reduction) was observed, along with mean 1.5 ± 0.1 $\log_{10}$ reduction in HBeAg and 1.3 ± 0.1 $\log_{10}$ reduction in HBcrAg (Fig. 1, E and F). HBsAg in HBeAg-negative cohort 7 patients decreased to a similar degree as in NUC-experienced HBeAg-negative patients in cohort 4, but after a delay of about 3 weeks (Fig. 1G). We have no explanation for this delayed response, but it may be a secondary effect of knockdown of other viral components on HBsAg expression. The transitional HBeAg-positive patient demonstrated HBsAg reductions intermediate to those observed in HBeAg-positive and HBeAg-negative patients in cohort 7. Together, these results suggested that HBeAg negativity and previous long-term NUC therapy adversely affected the ability of ARC-520 to reduce expression of HBsAg.

Differential HBsAg reduction in response to ARC-520 is associated with HBeAg status in chronically infected chimpanzees

In addition to the Heparc-2001 clinical trial, we conducted a study of ARC-520 in chimpanzees chronically infected with HBV. Nine CHB chimpanzees were available for inclusion in this study: five males and

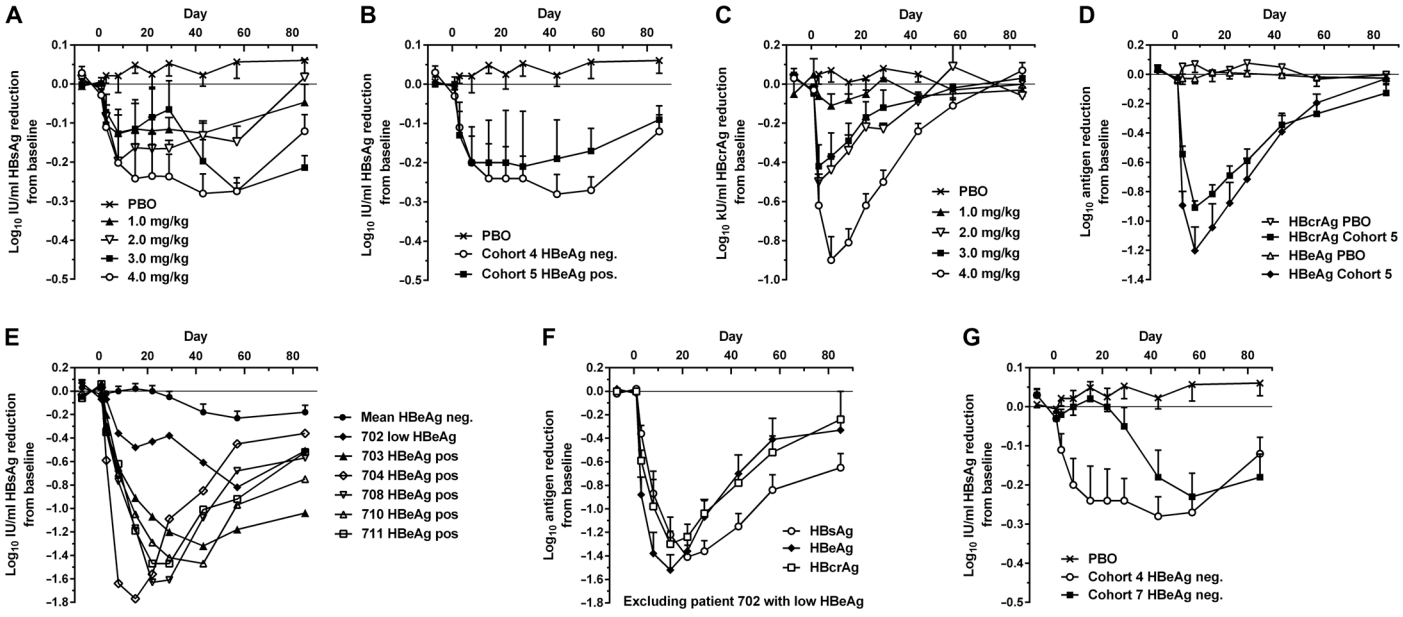

Fig. 1. Serum HBsAg, HBcrAg, and HBeAg reduction in human patients treated with a single dose of ARC-520. CHB patients were given a single intravenous dose of ARC-520 (1 to 4 mg/kg) on a background of daily oral NUCs. HBsAg (**A**) or HBcrAg (**C**) reduction in CHB patients who were NUC-experienced HBeAg-negative and received single doses (1 to 4 mg/kg) (cohorts 1 to 4, $n = 6$). (**B**) HBsAg reduction in CHB patients who were NUC-experienced HBeAg-negative (cohort 4, $n = 6$) or NUC-experienced HBeAg-positive (cohort 5, $n = 6$) who received a single dose (4 mg/kg). (**D**) HBcrAg and HBeAg reduction in CHB patients who were NUC-experienced HBeAg-positive and received a single dose (4 mg/kg) (cohort 5, $n = 6$). (**E**) HBsAg reduction for individual CHB patients who were NUC-naïve HBeAg-positive and received a single dose (4 mg/kg) in cohort 7 ($n = 6$). (**F**) HBsAg, HBeAg, and HBcrAg reductions in CHB patients who were NUC-naïve HBeAg-positive and received a single dose (4 mg/kg) (cohort 7, $n = 5$). (**G**) HBsAg reduction in CHB patients who were HBeAg-negative and NUC-naïve (cohort 7, $n = 6$) or NUC-experienced (cohort 4, $n = 6$). PBO, patients on NUC therapy given placebo injection. Error bars show SEM.

four females, five initially HBeAg-positive and four HBeAg-negative (table S4). Safety and efficacy of repeat dosing of the chimpanzees with ARC-520 were monitored with regular blood collections for evaluation of safety parameters and HBV serum DNA, HBsAg, HBeAg, and anti-HBsAg and anti-HBeAg antibodies. Initial HBsAg expression varied by four orders of magnitude, and production of HBV serum DNA by more than six orders of magnitude, providing an opportunity to evaluate the breadth of ARC-520 efficacy.

The chimpanzees were treated with daily oral NUCs (ETV for all, and for chimpanzee 4x0139 ETV + tenofovir) for 8 to 24 weeks to reduce viral replication before dosing with ARC-520 (Fig. 2A). While continuing NUC treatment, the chimpanzees were then given ARC-520 once every 4 weeks (Q4W) for a total of 6 to 11 injections. Monitoring of clinical chemistry and hematology parameters throughout the study showed that treatment with ARC-520 and NUCs was well tolerated with no observed toxicity (table S8).

Mean serum HBV DNA production in HBeAg-positive chimpanzees decreased by 4.0 ± 0.2 $\log_{10}$ copies/ml during NUC lead-in (Fig. 2B). All HBeAg-negative chimpanzees had quantities of serum DNA close to the lower limit of detection that became undetectable after 2 weeks of NUC treatment. After NUC lead-in, the first ARC-520 injection reduced mean HBV serum DNA by an additional 1.3 ± 0.1 $\log_{10}$ in HBeAg-positive chimpanzees (Fig. 2B). HBV DNA continued to be suppressed during ARC-520 treatment to the degree observed at nadir after the first dose. Two chimpanzees initially HBeAg-positive, 89A008 and A4A014, seroconverted to HBeAg-negative during the study, and their serum HBV DNA becomes undetectable.

HBeAg expression changed negligibly during NUC lead-in, with the exception of HBeAg transitional chimpanzee 89A008 that seroconverted for HBeAg during NUC lead-in (Fig. 2C). In the 40 days between the health check and start of NUC lead-in, HBeAg expression in 89A008 decreased fivefold and then continued to decline 3.5 $\log_{10}$ ng/ml during the 20-week NUC lead-in. In the other four HBeAg-positive chimpanzees, mean HBeAg expression was reduced by 1.0 ± 0.1 $\log_{10}$ after the first ARC-520 injection and remained suppressed to a similar degree throughout ARC-520 dosing, although HBeAg expression partially rebounded from nadir after each injection (Fig. 2C). Chimpanzee A4A014 became positive for anti-HBe antibodies, and then HBeAg became undetectable after the fifth ARC-520 injection.

At study initiation, HBsAg expression was an average of 19-fold higher in the HBeAg-positive than HBeAg-negative chimpanzees (table S4). Two HBeAg-negative chimpanzees (88A010 and 95A010) produced amounts of HBsAg similar to those of the two HBeAg-positive chimpanzees that seroconverted for HBeAg during the study (A4A014 and 89A008), whereas the other two HBeAg-negative chimpanzees produced two orders of magnitude less (4x0506 and 95A008). HBsAg expression decreased minimally during NUC lead-in (Fig. 2, D and E). HBeAg-positive animals responded to the first dose of ARC-520 (2 to 4 mg/kg) with HBsAg reductions of 0.9 to 1.4 $\log_{10}$ 4 weeks after injection, whereas the HBeAg-negative chimpanzees responded less well, with 0.4 to 0.7 $\log_{10}$ reductions at nadir (Fig. 2D). The extent of HBsAg knockdown appeared not to correlate with production of HBsAg at start of study, but rather with HBeAg status (Fig. 2E). Unlike the more steady degree of HBV DNA and HBeAg suppression, HBsAg expression gradually decreased throughout the ARC-520 dosing period regardless of HBeAg status, with the exception of A3A006 (Fig. 2, D and E).

As observed in human patients who had been NUC-naïve before dosing with ARC-520, HBeAg-positive chimpanzees responded with much deeper knockdown than HBeAg-negative chimpanzees. Mean HBsAg values normalized to ARC-520 dosing day 1 are shown in

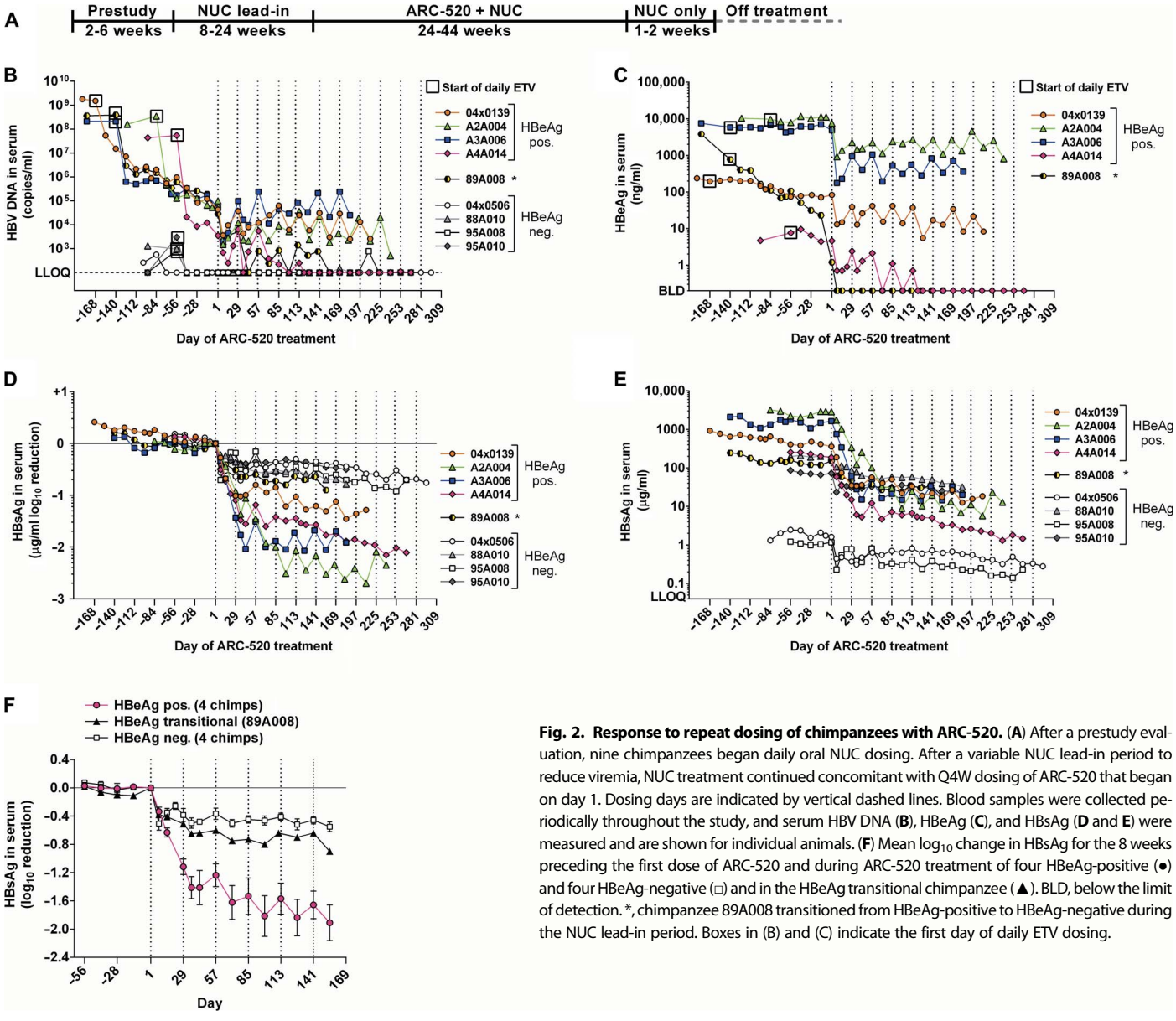

Fig. 2. Response to repeat dosing of chimpanzees with ARC-520. (**A**) After a prestudy evaluation, nine chimpanzees began daily oral NUC dosing. After a variable NUC lead-in period to reduce viremia, NUC treatment continued concomitant with Q4W dosing of ARC-520 that began on day 1. Dosing days are indicated by vertical dashed lines. Blood samples were collected periodically throughout the study, and serum HBV DNA (**B**), HBeAg (**C**), and HBsAg (**D** and **E**) were measured and are shown for individual animals. (**F**) Mean $\log_{10}$ change in HBsAg for the 8 weeks preceding the first dose of ARC-520 and during ARC-520 treatment of four HBeAg-positive (●) and four HBeAg-negative (□) and in the HBeAg transitional chimpanzee (▲). BLD, below the limit of detection. *, chimpanzee 89A008 transitioned from HBeAg-positive to HBeAg-negative during the NUC lead-in period. Boxes in (B) and (C) indicate the first day of daily ETV dosing.

Fig. 2F. HBsAg knockdown after ARC-520 injection in the three chimpanzees that remained HBeAg-positive throughout the study (4x0139, A2A004, and A3A006) was similar to that in A4A014, which became HBeAg-negative, and there were no apparent differences in effect between 2 and 4 mg/kg of ARC-520 (Fig. 2, D to F). HBsAg reductions after ARC-520 treatment of HBeAg transitional chimpanzee 89A008 were intermediate between the HBeAg-negative and HBeAg-positive chimpanzees (Fig. 2, D to F), reminiscent of the HBsAg reduction in the low HBeAg–expressing patient 702 from Heparc-2001 cohort 7 (Fig. 1E).

Abundance and characteristics of HBV DNA and RNA in the liver differ between HBeAg-positive and HBeAg-negative chimpanzees

To understand the reason for the differential response to ARC-520 between HBeAg-positive and HBeAg-negative chimpanzees, and potentially by extension in HBeAg-positive and HBeAg-negative humans, we characterized the molecular genetics of HBV found in these two chimpanzee serotypes. Liver biopsies were performed on eight of the chimpanzees at the prestudy health check, after NUC lead-in on day 1, and at various time points after ARC-520 injections. These specimens were divided for isolation of total liver DNA and total liver RNA and for histological evaluation of paraffin-embedded tissue. Chimpanzee 4x0506 was not biopsied because of low prestudy platelet counts.

Prestudy quantities of total HBV DNA in the liver were measured using quantitative polymerase chain reaction (qPCR) with a probe in the core region. The HBeAg-positive chimpanzees had 5.9 to 7.8 $\log_{10}$ copies of HBV/μg of host DNA, whereas the HBeAg-negative chimpanzees had considerably less (3.6 to 4.4 $\log_{10}$ copies/μg) (fig. S4), consistent with the lower serum DNA production in HBeAg-negative chimpanzees. NUC treatment alone during lead-in reduced total HBV liver DNA in the HBeAg-positive chimpanzees by an average of 0.45 ± 0.06 $\log_{10}$ per

month but did not reduce it in the HBeAg-negative chimpanzees, suggesting that the majority of HBV DNA in the liver of the latter is not dependent on replication via viral polymerase.

Total HBV DNA includes cccDNA, replication products such as rcDNA, and integrated HBV. To evaluate the molecular form of HBV DNA species in the livers, the biopsy samples were treated with Plasmid-Safe ATP-Dependent DNase (PSD) before qPCR. PSD was developed to digest contaminating sheared chromosomal DNA in plasmid DNA preparations (Epicentre Technologies). PSD has its greatest activity on fragments of double-stranded DNA and, to a lesser degree, digests single-stranded DNA; thus, it is expected to be most active on integrated HBV DNA and, to a lesser degree, on HBV replication intermediates including rcDNA. cccDNA is expected to be resistant to digestion by PSD. We observed that PSD digestion decreased liver HBV DNA in HBeAg-positive chimpanzee samples by 14 ± 3–fold in the prestudy samples but by only 1.8 ± 0.2–fold after the NUC lead-in, suggesting a change in the number and/or form of replication products in these animals treated with NUCs (fig. S4). In contrast, HBV DNA in HBeAg-negative chimpanzees was more sensitive to PSD digestion during NUC treatment alone (43 ± 21–fold decrease). These results, along with the significantly lower HBV liver DNA levels that did not decrease during NUC treatment, could be explained by a greater proportion of HBV genomes being integrated in HBeAg-negative compared to HBeAg-positive chimpanzees. HBV is known to integrate into host chromosomal DNA, and human CHB patients are known to have an increasing number of HBV integrants as the infection progresses (*7*).

Paired-end sequencing of fragmented liver DNA enriched for HBV-containing sequences revealed that HBeAg-positive and HBeAg-negative chimpanzees had HBV DNA integrated into their genomes (fig. S5). The primary source of integrated HBV DNA is dslDNA, an in situ primed, aberrant replication product that results when the cap-containing RNA primer fails to translocate to the downstream direct repeat 2 (DR2) sequence during plus strand DNA synthesis (*9*). The upstream end of dslDNA is at DR1, and the downstream end terminates in the gap region between DR2 and DR1, the majority ending proximal to DR1 (fig. S1) (*5*, *22*). Consistent with this mechanism of HBV integration, the major integration sites in our study chimpanzees were at DR1. HBeAg-negative chimpanzee 88A010 (25 years old), transitional 89A008 (24 years old), and HBeAg-positive 4x0139 (37 years old) had the highest number of integration events, whereas HBeAg-positive A4A014 (the youngest at 9 years old) had the lowest, suggesting a possible increase in integrated HBV DNA with duration of infection as observed in humans (*7*). Integrated HBV DNA in 4x0139 was previously characterized, with results showing a pattern of integration similar to that seen in our study (*23*).

HBV transcripts in the liver were evaluated by three distinct approaches, each of which provides somewhat different but complementary information. These were reverse transcription qPCR (RT-qPCR), paired-end next-generation mRNA sequencing (mRNA-seq), and single-molecule real-time (SMRT) sequencing (Iso-seq). Total HBV transcripts in the liver specimens were quantified using an RT-qPCR probe in the X gene (X probe) that hybridized to a region expected to be in all cccDNA-derived transcripts (precore, pgRNA, pre-S1, pre-S2/S, and X). The number of HBV transcripts in three HBeAg-positive chimpanzees was compared to that in three HBeAg-negative chimpanzees (Fig. 3A). HBeAg-positive chimpanzee 4x0139 was omitted because of low X probe efficiency in this animal, and 89A008 was omitted because it was transitioning to HBeAg-negative status. The mean number of total transcripts was 18-fold higher in HBeAg-positive chimpanzees (7.8 to 8.7 $\log_{10}$ copies/μg of RNA) than in HBeAg-negative chimpanzees (6.6 to 7.6 $\log_{10}$ copies/μg), similar to the difference in HBsAg expression between these groups. Short-term treatment with NUCs is not expected to exert an effect on the level of transcripts, and in both groups of chimpanzees, total HBV transcripts were not significantly different at prestudy from those after NUC lead-in (Fig. 3A). Consistent with reduction of HBsAg, 1 week after the second ARC-520 injection (day 36), total HBV RNA (with X probe) was reduced 89 ± 2% in three HBeAg-positive chimpanzees and 62 ± 4% in the HBeAg-negative chimpanzees. The difference in RNA reduction was similar to the difference in HBsAg reduction observed in these two groups of chimpanzees at this time point (Fig. 2F). HBeAg-positive chimpanzee 4x0139 was omitted from this analysis because the X probe appears to be less efficient in this animal: The core probe detected about 100 times more transcripts than the X probe. Given the high level of HBsAg production in this chimpanzee, it is unlikely that the HBsAg transcripts comprise less than 1% of the total, as assay results using this probe would suggest.

The precore plus pgRNA transcripts can be distinguished from the total HBV transcripts using a qPCR probe to a conserved sequence in the core region (Fig. 3B). The precore/pgRNA transcripts comprised only 3.5 ± 0.5% of the total HBV transcripts in HBeAg-negative chimpanzees, whereas they comprised 52.6 ± 0.5% of the total in HBeAg-positive chimpanzees.

Unlike PCR, which requires knowledge of target site sequences and is less efficient on variants with mismatches to primer or probe, mRNA-seq analysis accommodates variation (*24*). Using liver biopsy samples collected after NUC lead-in, about 40 million sequencing reads with a length of 50 bases were generated from each total liver RNA sample.

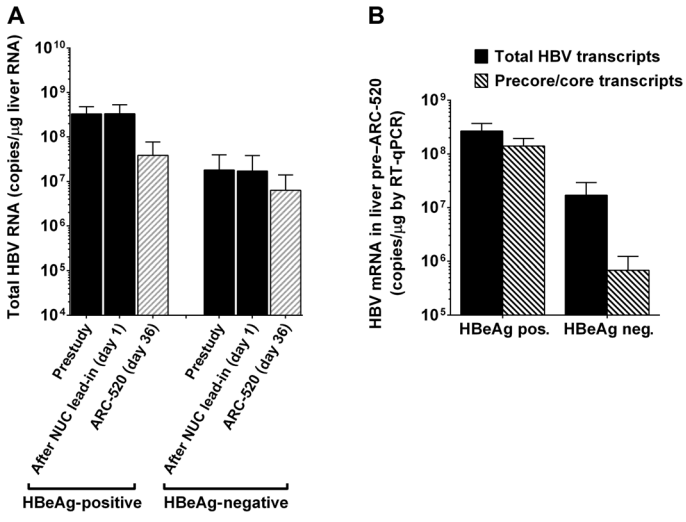

Fig. 3. Serum HBsAg and liver HBV mRNA reduction in chimpanzees dosed with ARC-520. After prestudy evaluation, nine chimpanzees began NUC dosing for a lead-in period of 8 to 24 weeks. Q4W dosing with ARC-520 began on day 1. Liver mRNA from biopsies of HBeAg-positive chimpanzees (A2A004, A3A006, and A4A014) and HBeAg-negative chimpanzees (88A010, 95A008, and 95A010) was evaluated for HBV gene expression by RT-qPCR with probe sets in core to measure the amount of precore mRNA/pgRNA and in X to measure total HBV mRNA. (**A**) Mean total HBV mRNA amounts were compared between HBeAg-positive and HBeAg-negative chimpanzees before study, after the NUC lead-in (day 1), and 1 week after the second ARC-520 injection (day 36). (**B**) The numbers of total HBV transcripts and precore/pgRNA transcripts on day 1 are compared for the HBeAg-positive and HBeAg-negative chimpanzees. Error bars show SEM.

Histograms were generated by aligning the reads from each chimpanzee to its consensus HBV DNA sequence obtained from liver DNA sequencing (Fig. 4). A steep decrease in the number of reads just downstream of the major HBV PAS (sequence TATAAA) in HBeAg-positive chimpanzees suggests that the majority of HBV transcripts terminate near this PAS. In the HBeAg-negative chimpanzees, few reads extended beyond DR1, and thus, they lacked the major HBV PAS that is located 81 bases downstream of DR1. There was no indication of resistance to ARC-520 developing, as the dominant sequences at the siRNA target sites, in those transcripts that contained them, remained similar before and after multiple ARC-520 doses, and HBV RNA remained suppressed (table S5 and fig. S6). These mRNA-seq results are consistent with HBsAg transcripts in HBeAg-negative chimpanzees being produced from integrated dslDNA.

We performed Iso-seq to allow sequencing of the entire full-length complementary DNA, using total liver RNA from one HBeAg-positive (A2A004) and one HBeAg-negative (88A010) chimpanzee. Alignment of the sequencing data from A2A004 to the HBV genome revealed that the vast majority (90.5%) of S transcripts had the expected 5′ and 3′ ends, originating from the expected promoters and terminating at the HBV PAS, respectively (Fig. 5A). In contrast, the 5′ ends of S transcripts from animal 88A010 mapped to the S promoters, but in most cases, the 3′ ends failed to align to HBV beginning in the DR2-DR1 region upstream of the HBV PAS (Fig. 5B). These were hybrid transcripts containing HBV sequence fused to non-HBV sequences. Most HBV transcripts in HBeAg-negative 88A010 were fused to a chimpanzee sequence (66.4%), a HBV sequence (10.1%), or a sequence with unknown origin (0.9%). HBV-chimpanzee fusion transcripts in this animal used cryptic chimpanzee PASs identified as the sequence AATAAA or with a single base change (table S6). These sequences were observed within the 60 bases proximal to the poly(A) sequences. The most common PAS was AATAAA (17.7%), and the majority of transcripts (55.8%) had more than one putative PAS. These results demonstrate that fusion transcripts can use chimpanzee putative PAS sequences near their integration sites and do not require a bona fide HBV PAS.

The 3′ terminus of dslDNA is located between the DR2 and DR1 elements and excludes the major HBV PAS. As shown in fig. S1, an alternate PAS (sequence CATAAA) first detected in HCC tissue is located about 130 bases upstream of the major PAS (*25*). HBV RNA transcripts that terminate at the alternate PAS are referred to as truncated RNA (trRNA) (*26*, *27*). Some integrated HBV genomes derived from dslDNA could include this alternate PAS. This alternate PAS terminus was detected in 32.8% (42 of 128) of the nonfusion HBV transcripts in the HBeAg-negative chimpanzee, but only in 0.3% (7 of 2466) of the nonfusion transcripts in the HBeAg-positive chimpanzee.

If trRNA transcripts are produced from integrated HBV DNA, as was previously observed in HCC, we would expect them to encode HBsAg but not HBeAg, core, or polymerase, because the upstream and adjacent precore/core promoter is deleted in integrated dslDNA. Consistent with this hypothesis, we observed a significant amount of trRNA encoding HBsAg in the HBeAg-negative chimpanzee liver RNA along with a majority of transcripts that used a PAS from the host genome.

Although 90.5% of the HBV transcripts in A2A004 were nonfusion, only 22.7% were nonfusion from HBeAg-negative 88A010 (Table 1). Consistent with our DNA-seq and mRNA-seq results, the Iso-seq data also demonstrate that HBV-chimpanzee integration points are located

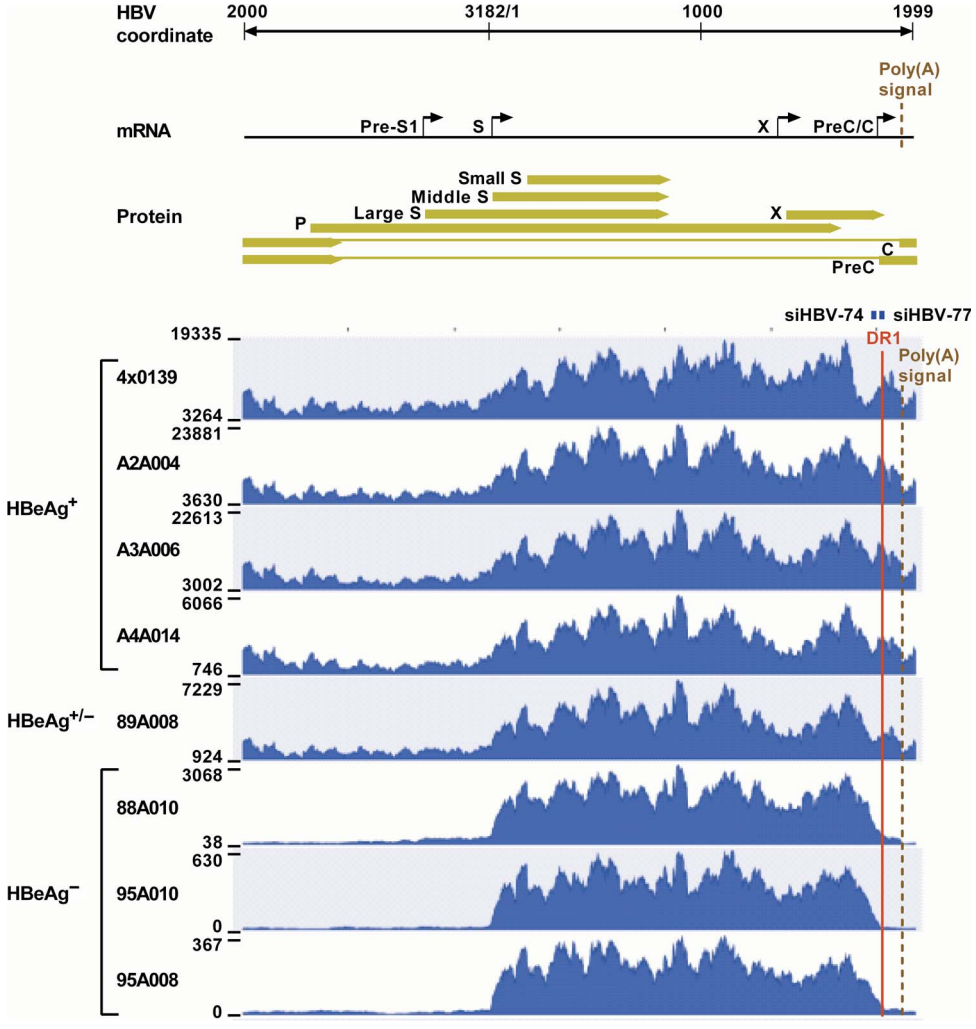

Fig. 4. Liver HBV mRNA paired-end sequencing reads in HBeAg-positive and HBeAg-negative chimpanzees. The HBV mRNA and HBV protein open reading frames are positioned relative to the coordinates of the HBV genome. The mRNA-seq read histograms are shown for HBeAg-positive chimpanzees 4x0139, A2A004, A3A006, and A4A014; for HBeAg transitional chimpanzee 89A008; and for HBeAg-negative chimpanzees 88A010, 95A010, and 95A008. Locations of the DR1 sequence (red line), HBV PAS (brown dashed line), and binding sites for the siRNAs in ARC-520 (siHBV-74 and siHBV-77) are indicated.

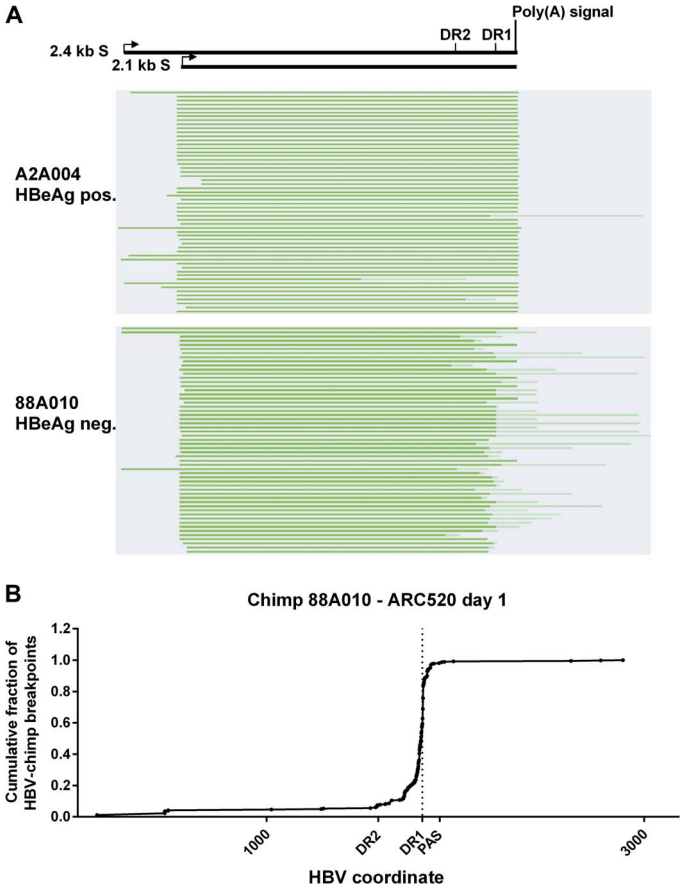

Fig. 5. Mapping of HBV S transcripts from HBeAg-positive and HBeAg-negative chimpanzees. Total RNA isolated from the liver biopsies after the NUC lead-in and before ARC-520 dosing on day 1 from HBeAg-positive chimpanzee A2A004 and HBeAg-negative chimpanzee 88A010 was reverse-transcribed, size-selected, and sequenced with SMRT sequencing. (**A**) Full-length nonconcatemer reads were aligned to each chimpanzee's consensus HBV DNA sequence. Green lines represent HBV-containing transcripts. Dark green represents sequences aligning to HBV, and light green represents those not aligning to HBV. The HBV coordinates are shown with elements DR2, DR1, and the HBV PAS. (**B**) Cumulative fraction of HBV-chimpanzee breakpoints was plotted against the HBV coordinate.

primarily near DR1. A significant portion of these transcripts lack the target sites for the RNAi triggers in ARC-520.

Deep reduction of HBsAg was observed in HBeAg-negative chimpanzees treated with siRNA targeting outside the DR1-DR2 region

We tested the hypothesis that the reason for less efficient ARC-520–mediated HBsAg reduction in HBeAg-negative chimpanzees was due to loss of ARC-520 siRNA target sites in the mRNA encoding their HBsAg. Two HBeAg-negative chimpanzees were treated with siRNA siHBV-75 that targets a site upstream of the DR1-DR2 region. The other two chimpanzees continued to receive ARC-520. After the 10th dose of ARC-520, chimpanzees 4x0506 and 95A008 both had 0.7 $\log_{10}$ reduction of HBsAg relative to day 1. After seven doses of ARC-520, chimpanzees 88A010 and 95A010 had 0.8 and 0.5 $\log_{10}$ HBsAg reduction, respectively. These two chimpanzees were then dosed three times (Q4W) with siHBV-75 (4 mg/kg). The HBsAg was reduced by 1.4 and 1.7 $\log_{10}$, 1.9 and 2.4 $\log_{10}$, and finally 2.3 and 3.0 $\log_{10}$ relative to day 1 after each of the three successive siHBV-75 doses in 88A010 and 95A010, respectively (Fig. 6). These reductions demonstrated that HBsAg could be just as effectively reduced by RNAi in the HBeAg-negative chimpanzees as in the HBeAg-positive chimpanzees, as long as the target site for the siRNA was present in the mRNA. HBeAg-negative 88A010 and transitional 89A008 both had populations of hepatocytes in liver biopsies that appeared to be clonal and stained strongly for accumulated HBsAg, highly suggestive of integrated HBV (fig. S7). This HBsAg staining was greatly reduced after treatment with siHBV-75.

DISCUSSION

The differential response to RNAi therapeutic ARC-520 reflected in the lower magnitude of HBsAg knockdown in HBeAg-negative or NUC-experienced HBeAg-positive CHB patients in comparison to NUC-naïve HBeAg-positive CHB patients could not have been predicted based on current models, which assume that cccDNA is the only significant source of HBV transcripts. The fact that patients in cohort 7 initiated NUC therapy on day 1, in contrast to the patients in the other cohorts that were NUC-experienced, also cannot explain these results, as it has been previously established that NUCs do not significantly affect HBsAg expression (*28*). Instead, our data point to an additional, previously underrecognized source of HBsAg, namely, integrated HBV DNA. Evidence for this comes from a variety of observations as well as direct experimentation. In humans, we show that the minimal HBsAg knockdown by ARC-520 in poor responders is not due to an inherent inefficiency of the RNAi machinery, because knockdown of HBcrAg in these patients was similar in magnitude to HBsAg knockdown in NUC-naïve HBeAg-positive patients. HBcrAg transcripts can only be produced from HBV DNA in which the precore/core promoters are upstream and adjacent to the coding region. This is the spatial arrangement found in cccDNA, but not in integrated HBV DNA, hinting that HBcrAg and HBsAg may come from different HBV DNA sources. HBeAg data in NUC-treated and NUC-naïve HBeAg-positive patients were consistent with this conclusion.

The availability of chronically infected chimpanzees, which also showed a differential pattern of response in HBeAg-negative versus HBeAg-positive serotypes, allowed us to perform a series of investigations to more directly examine the molecular basis for this phenomenon. First, we showed that total liver HBV DNA was present at lower quantities in HBeAg-negative chimpanzees compared to HBeAg-positive chimpanzees, and the amount of HBV DNA was largely unchanged by NUCs. This suggests that the majority of the liver HBV DNA in these HBeAg-negative chimpanzees was not dependent on active HBV replication but rather represented HBV DNA integrated into the host chromosome. Second, we demonstrated that the proportion of precore/pgRNA transcripts, expected to arise from cccDNA, to the total amount of HBV transcripts was minimal in HBeAg-negative chimpanzees, suggesting that most transcripts were produced from non-cccDNA such as integrated HBV DNA in the chimpanzees with this serotype. These data were confirmed using mRNA-seq, which additionally revealed that HBV sequences ended before the HBV PAS in the vast majority of transcripts in HBeAg-negative animals. This points to transcription from integrated HBV DNA, which has 3′ sequence deletions that would include deletion of the HBV PAS, and is consistent with our mapping of chimpanzee/HBV breakpoints in integrated HBV DNA. Third, sequencing of full-length HBV transcripts from the liver of an HBeAg-negative chimpanzee revealed that most were fused to host

Table 1. Characterization of HBV transcripts and PAS sequences in HBeAg-negative and HBeAg-positive chimpanzees. Total liver RNA collected after the NUC lead-in and before ARC-520 dosing (day 1) from HBeAg-negative chimpanzee 88A010 and HBeAg-positive chimpanzee A2A004 was sequenced with the SMRT approach. All mRNA sequences that could be at least partially aligned with the HBV genome were analyzed to determine the number that contained entirely HBV sequence, HBV-chimpanzee fusion sequence, HBV-HBV fusion sequence, or HBV fused to an unknown sequence.

Characterization of HBV transcripts

	HBeAg-negative 88A010		HBeAg-positive A2A004	
HBV transcripts	**Number of transcripts**	**Percentage**	**Number of transcripts**	**Percentage**
HBV nonfusion	128	22.7	2466	90.5
HBV-chimpanzee	375*	66.4	35†	1.3
HBV-HBV	57	10.1	218‡	8.0
HBV-other	5	0.9	7	0.3
Total	565	100	2726	100

Analysis of PAS sequences in nonfusion HBV transcripts

	HBeAg-negative 88A010		HBeAg-positive A2A004	
PAS sequence	**Number of transcripts**	**Percentage**	**Number of transcripts**	**Percentage**
TATAAA	80	62.5	2396	97.2
CATAAA	42	32.8	7§	0.3
Other	1	0.8	18	0.7
None detected	5	3.9	45	1.8
Total	128	100	2466	100

*Thirteen reads with reverse orientation were excluded from further analysis. †Two reads with reverse orientation were excluded from further analysis, and 12 transcripts with poly(A) or poly(T) appear to have been misidentified as fusion transcripts. ‡One hundred sixty-six transcripts contain gaps in HBV sequence consistent with splicing (*39*). §Two of seven could be mutants or sequencing errors (TATAAA expected based on the HBV coordinate).

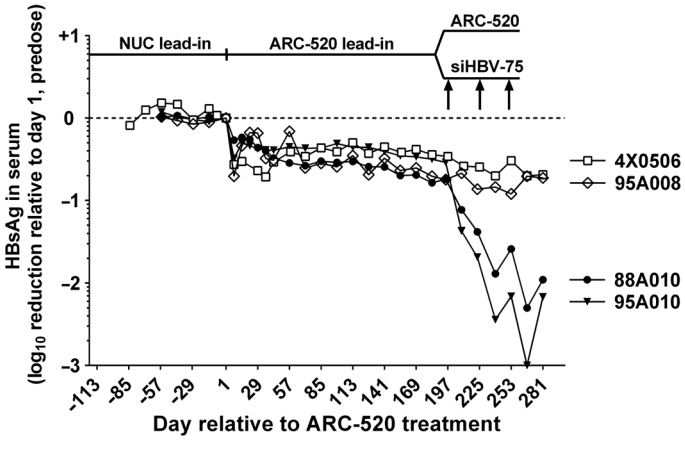

Fig. 6. Treatment of HBeAg-negative chimpanzees with siRNA targeted outside the DR1-DR2 region. After a NUC lead-in, all four HBeAg-negative chimpanzees were given seven Q4W doses of ARC-520. Chimpanzees 4x0506 and 95A008 were then given an additional three doses of ARC-520 (4 mg/kg), whereas 95A010 and 88A010 were given three doses of siHBV-75 (4 mg/kg) plus ARC-EX1 (4 mg/kg) delivery reagent. HBsAg in serum was measured.

chimpanzee sequence and that these fusion points fell between DR1 and DR2, which would be expected if they were expressed from integrated HBV DNA. Deletion of HBV sequences in this region may include the target sequences for the RNAi triggers in ARC-520, depending on the extent of the deletion. Our Iso-seq data showed that this was the case in the HBeAg-negative chimpanzee. This would explain the decrease in HBsAg knockdown observed in HBeAg-negative chimpanzees relative to HBeAg-positive chimpanzees in which the vast majority of HBV transcripts contained the target sites. Finally, treatment with an RNAi trigger that targeted a sequence upstream of these deletions resulted in a degree of HBsAg knockdown in HBeAg-negative chimpanzees that was comparable to that in HBeAg-positive chimpanzees. Although minor variations in the process of HBV DNA integration may exist between humans and chimpanzees, our mapping data and those presented by others suggest that the processes are remarkably similar (*22*, *23*, *29*). We interpret the data in toto to indicate that integrated HBV DNA is a substantial source of HBsAg in HBeAg-negative chimpanzees, HBeAg-negative patients, and NUC-experienced HBeAg-positive patients with low cccDNA.

Despite the well-documented occurrence of HBV DNA integration, only minimal, if any, HBsAg was thought to be produced from integrated HBV DNA. However, integrated HBV DNA has been detected in HBsAg-positive individuals with no detectable HBV serum DNA (*30*). Others previously described in histological liver samples from CHB patients that the hepatocytes that stained for HBsAg were distinct from those that stained for core (*31*), and HBsAg-containing hepatocytes were often in clusters, consistent with clonal populations (*32*). We also observed prominent HBsAg staining suggestive of clonal

hepatocyte populations in an HBeAg-negative chimpanzee and the HBeAg transitional chimpanzee, but not in the HBeAg-positive chimpanzees. These data could be explained by significant HBsAg expression from integrated HBV DNA without actively transcribed cccDNA in the same hepatocytes. Tu *et al.* demonstrated that such clonal populations harboring integrated HBV DNA cannot result from random hepatocyte turnover but rather have a selective advantage that is not due to preneoplasia (*22*). Although the reason for this advantage is not completely understood, many of the clones in that study were shown to contain HBsAg. Having a means of producing HBsAg that is not dependent on viral replication or production of other potentially antigenic viral proteins may help sustain suppression of the immune system and allow for continued virion production. A single HBV genome can lead to infection of every hepatocyte (*33*). Thus, just a few cccDNA-containing cells able to escape immunosurveillance can maintain chronic infection and only complete immune control of HBsAg can be expected to prevent reinfection and result in a functional cure.

Integrated HBV DNA as a source of HBsAg may also help explain why amounts of HBsAg and serum HBV DNA correlate in untreated HBeAg-positive, chronically HBV infected individuals, particularly those with high HBV serum DNA, but correlate less well or not at all in HBeAg-negative patients and in those on NUC therapy (*34*–*37*). If integrated DNA produces HBsAg, then its production would be relatively independent of HBV DNA replication and thus HBV serum DNA production, in line with a recent study showing minimal change of HBsAg expression despite achievement of undetectable cccDNA in patients treated with nucleos(t)ide analogs for more than 5 years (*37*). In addition, a low amount of cccDNA resulting from chronic NUC therapy in cohort 5 patients before treatment with ARC-520 would explain the more limited HBsAg knockdown achieved in these HBeAg-positive patients relative to HBeAg-positive patients in cohort 7, which had not been exposed to chronic NUC therapy. ARC-520 and NUCs might be expected to have synergistic activity on inhibition of cccDNA replenishment, as ARC-520 degrades pgRNA and viral proteins involved in replication, whereas NUCs directly inhibit replication, but this study was not designed to address potential synergism.

A limitation of this work is that the numbers of chimpanzees and treatment-naïve HBV-infected patients (cohort 7) in this study were relatively small. However, the reduction in HBsAg in response to ARC-520 in HBeAg-negative chimpanzees and humans were similar, as were the responses in HBeAg-positive chimpanzees and humans, and the magnitude of the differences dependent on HBeAg status was large and nonoverlapping.

Our finding that integrated HBV DNA can serve as a source of HBsAg has implications for design of next-generation antivirals to treat CHB. For example, that HBsAg appears to be produced from integrated HBV DNA rather than solely from cccDNA implies that eliminating cccDNA will likely not eliminate HBsAg. Immune control that prevents reinfection and allows clearance of the virus remains the desired endpoint. Loss of HBsAg is the more relevant biomarker of immune control. This is likely the case whether the HBsAg is produced from cccDNA or from integrated HBV DNA. In a virus as evolutionarily successful as HBV, the abundant production of HBsAg may serve a critical function in the maintenance of CHB.

The increased understanding of HBsAg dynamics during chronic infection gained by the current investigation will lead to enhanced opportunities to reduce HBsAg expression and potentially allow the host immune response to eliminate residual infected cells. Direct RNAi-mediated reduction of HBsAg in the liver has the potential to improve the prognosis for infected individuals, but should take into account both cccDNA and integrated HBV DNA.

MATERIALS AND METHODS

Study designs

Clinical trial Heparc-2001 (NCT 02065336)

The study aimed to determine the safety, tolerability, and pharmacological effect of ARC-520 in CHB patients with or without preceding chronic NUC treatment. Initially, patients receiving chronic ETV were enrolled sequentially into five cohorts, 8 subjects per cohort, and randomized with a 6:2 (active/placebo) ratio (table S1). Each subject was assigned to either active (ARC-520) or placebo (0.9% normal saline) treatment using a block randomization algorithm. After completion of cohort 4 and while cohort 5 was recruiting, the protocol was amended to add cohort 6 and subsequently cohort 7 in open-label fashion without placebo groups. Patient selection and additional study details are in the Supplementary Materials.

Blood samples were collected before dose and at specified times after dosing to determine safety, pharmacokinetic (cohorts 1 to 5), pharmacodynamic (cytokines and complement), and HBV serology parameters. Patients were pretreated with antihistamine (chlorpheniramine; 8 mg orally) 2 hours before treatment administration and continued (cohorts 1 to 6) or started (cohort 7) daily oral ETV on day 1 (0.5 mg/day orally), continuing throughout the study.

ARC-520, supplied by Arrowhead Pharmaceuticals, was administered as a single intravenous infusion at ascending doses of 1, 2, 3, and 4 mg/kg, administered intravenously by clinical staff at the infusion rate of 10 mg/min.

The study was performed in accordance with the 2008 Declaration of Helsinki and good clinical practice guidelines and was approved by the Institutional Review Board of the University of Hong Kong/Hospital Authority Hong Kong West Cluster (Queen Mary Hospital, Hong Kong) and the Joint Chinese University of Hong Kong–New Territories East Cluster Clinical Research Ethics Committee (Prince of Wales Hospital, Hong Kong). All subjects gave written informed consent before screening.

Chimpanzee study

This study aimed to determine the safety, tolerability, and pharmacological effect of ARC-520 in nine available HBsAg-positive CHB chimpanzees (*Pan troglodytes*), as shown in table S4. Characteristics of viral genomes are shown in table S7. Chimpanzees were treated with daily oral NUC for a lead-in period and then in conjunction with ARC-520 dosing (table S4). All chimpanzees were given oral ETV, 0.5 mg daily for lamivudine-naïve chimpanzees and 1.0 mg daily for chimpanzees with previous exposure to lamivudine. Beginning on study day 108 and continuing through the ARC-520 dosing period, chimpanzee 4x0139 was dosed in addition to ETV with daily tenofovir (300-mg pediatric formulation) to further reduce viral load in this high replicating chimpanzee (*38*). After NUC lead-in, chimpanzees were dosed with ARC-520 Q4W for 6 to 11 doses. Five to 10 min before ARC-520 dosing (4 mg/kg), chimpanzees were given a 50-mg intravenous bolus of diphenhydramine as a precautionary measure to avoid infusion reaction. Dosing with siHBV-75 + ARC-EX1 was performed identically to dosing with ARC-520. Blood samples were collected before dose and at specified times after dosing to determine clinical chemistry, hematology, and HBV serology parameters (Supplementary Materials). Animal experimentation was conducted according to the *Guide for the Care and Use of Laboratory Animals* and approved by the Institutional Animal Care

and Use Committees of the Southwest National Primate Research Center at the Texas Biomedical Research Institute and the New Iberia Research Center at the University of Louisiana at Lafayette.

RNAi triggers and ARC-EX1

ARC-520 comprises API-520, the Active Pharmaceutical Ingredient consisting of two equimolar cholesterol-conjugated RNAi triggers named "siHBV-74" and "siHBV-77" in a liquid solution, plus the novel delivery excipient ARC-EX1 containing hepatocyte-targeted *N*-acetylgalactosamine–conjugated melittin-like peptide in a powdered form (*21*). RNAi trigger siHBV-75 was previously described (*21*).

Statistical analyses

Data are means ± SEM. Statistical analyses were performed using Microsoft Excel 2013 and GraphPad Prism software version 6.0.

SUPPLEMENTARY MATERIALS

www.sciencetranslationalmedicine.org/cgi/content/full/9/409/eaan0241/DC1

Materials and Methods

Fig. S1. HBV sequence elements near DR1 and DR2.

Fig. S2. Serum HBsAg, HBeAg, and HBcrAg reduction in human patients treated with two doses of ARC-520 2 weeks apart.

Fig. S3. Reduction of HBV serum DNA in CHB patients treated with a single dose of ARC-520 on a background of NUCs.

Fig. S4. Quantitation of liver HBV DNA in chimpanzees.

Fig. S5. Mapping of HBV DNA integration sites.

Fig. S6. Massive paired-end sequencing of chimpanzee liver mRNA and alignment to HBV reference genome.

Fig. S7. Immunohistochemical staining of HBsAg in livers of HBeAg-positive and HBeAg-negative chimpanzees.

Table S1. Individual CHB patient demographics at screening and maximum HBsAg reduction from baseline in clinical trial Heparc-2001.

Table S2. Mean CHB patient demographics at screening and maximum HBsAg reduction from baseline in clinical trial Heparc-2001.

Table S3. Treatment-emergent adverse events in cohorts 1 to 7 of the Heparc-2001 study.

Table S4. Characteristics of chimpanzees chronically infected with HBV and treatment regimens.

Table S5. mRNA-seq data obtained from liver biopsies of chimpanzees chronically infected with HBV.

Table S6. PASs in HBV-chimpanzee fusion transcripts of HBeAg-negative chimpanzee 88A010.

Table S7. HBV genome characteristics determined from liver DNA sequencing of study chimpanzees.

Table S8. Primary data.

REFERENCES AND NOTES

1. GBD 2013 Mortality and Causes of Death Collaborators, Global, regional, and national age–sex specific all-cause and cause-specific mortality for 240 causes of death, 1990–2013: A systematic analysis for the Global Burden of Disease Study 2013. *Lancet* **385**, 117–171 (2015).
2. M.-F. Yuen, S. H. Ahn, D.-S. Chen, P.-J. Chen, G. M. Dusheiko, J.-L. Hou, W. C. Maddrey, M. Mizokami, W.-K. Seto, F. Zoulim, C.-L. Lai, Chronic hepatitis B virus infection: Disease revisit and management recommendations. *J. Clin. Gastroenterol.* **50**, 286–294 (2016).
3. R. P. Beasley, L.-Y. Hwang, C.-C. Lin, C.-S. Chien, Hepatocellular carcinoma and hepatitis B virus. A prospective study of 22 707 men in Taiwan. *Lancet* **318**, 1129–1133 (1981).
4. C. T. Bock, S. Schwinn, S. Locarnini, J. Fyfe, M. P. Manns, C. Trautwein, H. Zentgraf, Structural organization of the hepatitis B virus minichromosome. *J. Mol. Biol.* **307**, 183–196 (2001).
5. Z. Jiang, S. Jhunjhunwala, J. Liu, P. M. Haverty, M. I. Kennemer, Y. Guan, W. Lee, P. Carnevali, J. Stinson, S. Johnson, J. Diao, S. Yeung, A. Jubb, W. Ye, T. D. Wu, S. B. Kapadia, F. J. de Sauvage, R. C. Gentleman, H. M. Stern, S. Seshagiri, K. P. Pant, Z. Modrusan, D. G. Ballinger, Z. Zhang, The effects of hepatitis B virus integration into the genomes of hepatocellular carcinoma patients. *Genome Res.* **22**, 593–601 (2012).
6. V. Schlüter, M. Meyer, P. H. Hofschneider, R. Koshy, W. H. Caselmann, Integrated hepatitis B virus X and 3′ truncated preS/S sequences derived from human hepatomas encode functionally active transactivators. *Oncogene* **9**, 3335–3344 (1994).
7. M. J. F. Fowler, C. Greenfield, C.-M. Chu, P. Karayiannis, A. Dunk, A. S. F. Lok, C. L. Lai, E. K. Yeoh, J. P. Monjardino, B. M. Wankya, H. C. Thomas, Integration of HBV-DNA may not be a prerequisite for the maintenance of the state of malignant transformation. An analysis of 110 liver biopsies. *J. Hepatol.* **2**, 218–229 (1986).
8. D. K.-H. Wong, M.-F. Yuen, H. Yuan, S. S.-M. Sum, C.-K. Hui, J. Hall, C.-L. Lai, Quantitation of covalently closed circular hepatitis B virus DNA in chronic hepatitis B patients. *Hepatology* **40**, 727–737 (2004).
9. S. Staprans, D. D. Loeb, D. Ganem, Mutations affecting hepadnavirus plus-strand DNA synthesis dissociate primer cleavage from translocation and reveal the origin of linear viral DNA. *J. Virol.* **65**, 1255–1262 (1991).
10. K. Kakimi, M. Isogawa, J. Chung, A. Sette, F. V. Chisari, Immunogenicity and tolerogenicity of hepatitis B virus structural and nonstructural proteins: Implications for immunotherapy of persistent viral infections. *J. Virol.* **76**, 8609–8620 (2002).
11. M. T. Chen, J.-N. Billaud, M. Sällberg, L. G. Guidotti, F. V. Chisari, J. Jones, J. Hughes, D. R. Milich, A function of the hepatitis B virus precore protein is to regulate the immune response to the core antigen. *Proc. Natl. Acad. Sci. U.S.A.* **101**, 14913–14918 (2004).
12. D. R. Milich, J. E. Jones, J. L. Hughes, J. Price, A. K. Raney, A. McLachlan, Is a function of the secreted hepatitis B e antigen to induce immunologic tolerance in utero? *Proc. Natl. Acad. Sci. U.S.A.* **87**, 6599–6603 (1990).
13. C. Boni, P. Fisicaro, C. Valdatta, B. Amadei, P. Di Vincenzo, T. Giuberti, D. Laccabue, A. Zerbini, A. Cavalli, G. Missale, A. Bertoletti, C. Ferrari, Characterization of hepatitis B virus (HBV)-specific T-cell dysfunction in chronic HBV infection. *J. Virol.* **81**, 4215–4225 (2007).
14. S. F. Wieland, F. V. Chisari, Stealth and cunning: Hepatitis B and hepatitis C viruses. *J. Virol.* **79**, 9369–9380 (2005).
15. A. Bertoletti, C. Ferrari, Innate and adaptive immune responses in chronic hepatitis B virus infections: Towards restoration of immune control of viral infection. *Gut* **61**, 1754–1764 (2012).
16. C. Seeger, F. Zoulim, W. S. Mason, Hepadnaviruses, in *Fields Virology*, B. N. Fields, D. M. Knipe, P. M. Howley, Eds. (Wolters Kluwer Health/Lippincott Williams & Wilkins, 2007), chap. 76, pp. 2977–3030.
17. G.-A. Kim, Y.-S. Lim, J. An, D. Lee, J. H. Shim, K. M. Kim, H. C. Lee, Y.-H. Chung, Y. S. Lee, D. J. Suh, HBsAg seroclearance after nucleoside analogue therapy in patients with chronic hepatitis B: Clinical outcomes and durability. *Gut* **63**, 1325–1332 (2014).
18. M.-F. Yuen, D. K.-H. Wong, J. Fung, P. Ip, D. But, I. Hung, K. Lau, J. C.-H. Yuen, C.-L. Lai, HBsAg Seroclearance in chronic hepatitis B in Asian patients: Replicative level and risk of hepatocellular carcinoma. *Gastroenterology* **135**, 1192–1199 (2008).
19. H. L.-Y. Chan, V. W.-S. Wong, G. L.-H. Wong, C.-H. Tse, H.-Y. Chan, J. J.-Y. Sung, A longitudinal study on the natural history of serum hepatitis B surface antigen changes in chronic hepatitis B. *Hepatology* **52**, 1232–1241 (2010).
20. T. Schluep, J. Lickliter, J. Hamilton, D. L. Lewis, C.-L. Lai, J. Y. N. Lau, S. A. Locarnini, R. G. Gish, B. D. Given, Safety, tolerability, and pharmacokinetics of ARC-520 injection, an RNA interference-based therapeutic for the treatment of chronic hepatitis B Virus infection, in healthy volunteers. *Clin. Pharmacol. Drug Dev.* **6**, 350–362 (2017).
21. C. I. Wooddell, D. B. Rozema, M. Hossbach, M. John, H. L. Hamilton, Q. Chu, J. O. Hegge, J. J. Klein, D. H. Wakefield, C. E. Oropeza, J. Deckert, I. Roehl, K. Jahn-Hofmann, P. Hadwiger, H.-P. Vornlocher, A. McLachlan, D. L. Lewis, Hepatocyte-targeted RNAi therapeutics for the treatment of chronic hepatitis B virus infection. *Mol. Ther.* **21**, 973–985 (2013).
22. T. Tu, W. S. Mason, A. D. Clouston, N. A. Shackel, G. W. McCaughan, M. M. Yeh, E. R. Schiff, A. R. Ruszkiewicz, J. W. Chen, H. A. J. Harley, U. H. Stroeher, A. R. Jilbert, Clonal expansion of hepatocytes with a selective advantage occurs during all stages of chronic hepatitis B virus infection. *J. Viral Hepat.* **22**, 737–753 (2015).
23. W. S. Mason, H.-C. Low, C. Xu, C. E. Aldrich, C. A. Scougall, A. Grosse, A. Clouston, D. Chavez, S. Litwin, S. Peri, A. R. Jilbert, R. E. Lanford, Detection of clonally expanded hepatocytes in chimpanzees with chronic hepatitis B virus infection. *J. Virol.* **83**, 8396–8408 (2009).
24. Z. Wang, M. Gerstein, M. Snyder, RNA-Seq: A revolutionary tool for transcriptomics. *Nat. Rev. Genet.* **10**, 57–63 (2009).
25. C. Hilger, I. Velhagen, H. Zentgraf, C. H. Schröder, Diversity of hepatitis B virus X gene-related transcripts in hepatocellular carcinoma: A novel polyadenylation site on viral DNA. *J. Virol.* **65**, 4284–4291 (1991).
26. F. van Bömmel, A. Bartens, A. Mysickova, J. Hofmann, D. H. Krüger, T. Berg, A. Edelmann, Serum hepatitis B virus RNA levels as an early predictor of hepatitis B envelope antigen seroconversion during treatment with polymerase inhibitors. *Hepatology* **61**, 66–76 (2015).
27. Q. Su, S.-F. Wang, T.-E. Chang, R. Breitkreutz, H. Hennig, K. Takegoshi, L. Edler, C. H. Schröder, Circulating hepatitis B virus nucleic acids in chronic infection: Representation of differently polyadenylated viral transcripts during progression to nonreplicative stages. *Clin. Cancer Res.* **7**, 2005–2015 (2001).
28. M. Martinot-Peignoux, T. Asselah, P. Marcellin, HBsAg quantification to optimize treatment monitoring in chronic hepatitis B patients. *Liver Int.* **35** (suppl. 1), 82–90 (2015).

29. W. S. Mason, C. Liu, C. E. Aldrich, S. Litwin, M. M. Yeh, Clonal expansion of normal-appearing human hepatocytes during chronic hepatitis B virus infection. *J. Virol.* **84**, 8308–8315 (2010).
30. S. J. Hadziyannis, H. M. Lieberman, G. G. Karvountzis, D. A. Shafritz, Analysis of liver disease, nuclear HBcAg, viral replication, and hepatitis B virus DNA in liver and serum of HBcAg vs. anti-HBe positive carriers of hepatitis B virus. *Hepatology* **3**, 656–662 (1983).
31. N. V. Naoumov, B. C. Portmann, R. S. Tedder, B. Ferns, A. L. W. F. Eddleston, G. J. M. Alexander, R. Williams, Detection of hepatitis B virus antigens in liver tissue. A relation to viral replication and histology in chronic hepatitis B infection. *Gastroenterology* **99**, 1248–1253 (1990).
32. I.-J. Su, M.-Y. Lai, H.-C. Hsu, D.-S. Chen, P.-M. Yang, S.-M. Chuang, J.-L. Sung, Diverse virological, histopathological and prognostic implications of seroconversion from hepatitis B e antigen to anti-HBe in chronic hepatitis B virus infection. *J. Hepatol.* **3**, 182–189 (1986).
33. S. Asabe, S. F. Wieland, P. K. Chattopadhyay, M. Roederer, R. E. Engle, R. H. Purcell, F. V. Chisari, The size of the viral inoculum contributes to the outcome of hepatitis B virus infection. *J. Virol.* **83**, 9652–9662 (2009).
34. H. L.-Y. Chan, V. W.-S. Wong, A. M.-L. Tse, C.-H. Tse, A. M.-L. Chim, H.-Y. Chan, G. L.-H. Wong, J. J.-Y. Sung, Serum hepatitis B surface antigen quantitation can reflect hepatitis B virus in the liver and predict treatment response. *Clin. Gastroenterol. Hepatol.* **5**, 1462–1468 (2007).
35. A. J. V. Thompson, T. Nguyen, D. Iser, A. Ayres, K. Jackson, M. Littlejohn, J. Slavin, S. Bowden, E. J. Gane, W. Abbott, G. K. K. Lau, S. R. Lewin, K. Visvanathan, P. V. Desmond, S. A. Locarnini, Serum hepatitis B surface antigen and hepatitis B e antigen titers: Disease phase influences correlation with viral load and intrahepatic hepatitis B virus markers. *Hepatology* **51**, 1933–1944 (2010).
36. V. K. Karra, S. J. Chowdhury, R. Ruttala, S. K. Polipalli, P. Kar, Clinical significance of quantitative HBsAg titres and its correlation with HBV DNA levels in the natural history of hepatitis B virus infection. *J. Clin. Exp. Hepatol.* **6**, 209–215 (2016).
37. C.-L. Lai, D. Wong, P. Ip, M. Kopaniszen, W.-K. Seto, J. Fung, F.-Y. Huang, B. Lee, G. Cullaro, C. K. Chong, R. Wu, C. Cheng, J. Yuen, V. Ngai, M.-F. Yuen, Reduction of covalently closed circular DNA with long-term nucleos(t)ide analogue treatment in chronic hepatitis B. *J. Hepatol.* **66**, 275–281 (2017).
38. J. Petersen, V. Ratziu, M. Buti, H. L. A. Janssen, A. Brown, P. Lampertico, J. Schollmeyer, F. Zoulim, H. Wedemeyer, M. Sterneck, T. Berg, C. Sarrazin, M. Lutgehetmann, P. Buggisch, Entecavir plus tenofovir combination as rescue therapy in pre-treated chronic hepatitis B patients: An international multicenter cohort study. *J. Hepatol.* **56**, 520–526 (2012).
39. G. Sommer, T. Heise, Posttranscriptional control of HBV gene expression. *Front. Biosci.* **13**, 5533–5547 (2008).

Acknowledgments: We thank C. Anzalone for conceiving the chimpanzee study; K. Liu, R. Wu, G. Wong, V. Wong, and D. Martin for assistance with clinical trial conduct; J. Goetzmann, K. Brasky, and D. Hasselschwert for chimpanzee trial conduct; B. Guerra, H. Lee, L. Notvall-Elkey, and C. Johnson for chimpanzee sample analysis; J. Hegge and J. Klein for supervision of chimpanzee dosing; M. Littlejohn for chimpanzee HBV sequence analysis; the University of Wisconsin Biotechnology Center DNA Sequencing Facility for targeted DNA sequencing service; the Great Lakes Genomics Center of the University of Wisconsin at Milwaukee for Iso-seq library preparation and sequencing; A. Sinha and Basepair LLC for customized sequence data analysis; and K. Jackson, R. Walsh, and R. Peterson for additional data analysis. **Funding:** This work was supported by NIH grant P51-OD011133 from the Office of Research Infrastructure Programs/Office of the Director to the Southwest National Primate Research Center and by research grants from Arrowhead Pharmaceuticals to Texas Biomedical Research Institute and to the University of Hong Kong.
Author contributions: C.I.W. and D.L.L. designed and oversaw the chimpanzee study, analyzed data, and wrote the initial manuscript. M.-F.Y. and H.L.-Y.C. performed the clinical trial, analyzed clinical data, and reviewed the manuscript. R.G.G., S.A.L., C.-L.L., C.F., and J.Y.N.L. oversaw the clinical trial, analyzed clinical and chimpanzee data, and reviewed the manuscript. B.D.G., J.H., and T.S. initially designed the clinical trial, analyzed clinical and chimpanzee data, and reviewed the manuscript. Z.X. performed chimpanzee deep sequencing analysis and assisted in drafting the manuscript. R.E.L. oversaw the chimpanzee study, analyzed data, and reviewed the manuscript. D.C. conducted and oversaw chimpanzee sample assays. S.B.K. analyzed data and reviewed the manuscript.
Competing interests: C.I.W., D.L.L., Z.X., B.D.G., T.S., J.H., and S.B.K. are or were employees of Arrowhead Pharmaceuticals. R.G.G., S.A.L., C.-L.L., C.F., and J.Y.N.L. receive compensation from Arrowhead Pharmaceuticals. M.-F.Y., H.L.-Y.C., R.E.L., and D.C. performed work under contract with Arrowhead Pharmaceuticals.

Submitted 21 February 2017
Accepted 4 August 2017
Published 27 September 2017
10.1126/scitranslmed.aan0241

Citation: C. I. Wooddell, M.-F. Yuen, H. L.-Y. Chan, R. G. Gish, S. A. Locarnini, D. Chavez, C. Ferrari, B. D. Given, J. Hamilton, S. B. Kanner, C.-L. Lai, J. Y. N. Lau, T. Schluep, Z. Xu, R. E. Lanford, D. L. Lewis, RNAi-based treatment of chronically infected patients and chimpanzees reveals that integrated hepatitis B virus DNA is a source of HBsAg. *Sci. Transl. Med.* **9**, eaan0241 (2017).

Science Translational Medicine

RNAi-based treatment of chronically infected patients and chimpanzees reveals that integrated hepatitis B virus DNA is a source of HBsAg

Christine I. Wooddell, Man-Fung Yuen, Henry Lik-Yuen Chan, Robert G. Gish, Stephen A. Locarnini, Deborah Chavez, Carlo Ferrari, Bruce D. Given, James Hamilton, Steven B. Kanner, Ching-Lung Lai, Johnson Y. N. Lau, Thomas Schluep, Zhao Xu, Robert E. Lanford and David L. Lewis

Sci Transl Med **9**, eaan0241.
DOI: 10.1126/scitranslmed.aan0241

How hepatitis hangs around

Hepatitis B virus (HBV) infects the liver, and chronic infection can lead to cirrhosis or cancer. Wooddell *et al.* report the results of a phase 2 trial of a drug based on RNA interference, which was unable to reduce viral burden in certain subsets of patients. To determine the mechanism of this variable response, the researchers examined chronically infected chimpanzees that had been treated with the drug. They found evidence that viral antigen was being produced from integrated HBV transcripts that did not harbor the target sequence. This study uncovers a previously unappreciated source of viral antigen, which could inform disease pathogenesis and help guide development of future HBV treatments.

Science Translational Medicine (ISSN 1946-6242) is published by the American Association for the Advancement of Science, 1200 New York Avenue NW, Washington, DC 20005.